

High-Qf value and temperature stable Zn²⁺-Mn⁴⁺ cooperated modified cordierite-based microwave and millimeter-wave dielectric ceramics

Zhiyu Xiu¹, Minmin Mao^{1,*}, Zhilun Lu², Zhichao Huang¹, Zeming Qi³, Hadi Barzegar Bafrooei¹, Tao Zhou¹, Dawei Wang⁴, Huixing Lin⁵, Ehsan Taheri-nassaj⁶, Kaixin Song^{1,*}

1. *College of Electronic Information, Hangzhou Dianzi University, Hangzhou, 310018, China*
2. *School of Engineering and the Built Environment, Edinburgh Napier University, Edinburgh EH10 5DT, UK*
3. *National Synchrotron Radiation Laboratory, University of Science and Technology of China, Hefei, 230029, P. R. China*
4. *Shenzhen Institutes of Advanced Technology, Chinese Academy of Sciences, Shenzhen, 518055, China*
5. *Key Laboratory of Inorganic Functional Material and Device, Shanghai Institute of Ceramics, Chinese Academy of Sciences, Shanghai, 200050, China*
6. *Department of Materials Engineering, Faculty of Engineering, Tarbiat Modares University, Tehran, 14115-143, Iran*

* Corresponding Authors: kxsong@hdu.edu.cn; mmm@hdu.edu.cn

Abstract

Cordierite-based dielectric ceramics with a lower dielectric constant would have significant application potential as dielectric resonator and filter materials for future ultra-low-latency 5G/6G millimeter-wave and terahertz communication. In this article, the phase structure, microstructure and microwave dielectric properties of $\text{Mg}_2\text{Al}_{4-2x}(\text{Mn}_{0.5}\text{Zn}_{0.5})_{2x}\text{Si}_5\text{O}_{18}$ ($0 \leq x \leq 0.3$) ceramics are studied by crystal structure refinement, scanning electron microscope (SEM), the theory of complex chemical bonds and infrared reflectance spectrum. Meanwhile, complex double-ions coordinated substitution and two-phase complex methods were used to improve its $Q \times f$ value and adjust its temperature coefficient. The $Q \times f$ values of $\text{Mg}_2\text{Al}_{4-2x}(\text{Mn}_{0.5}\text{Zn}_{0.5})_{2x}\text{Si}_5\text{O}_{18}$ single-phase ceramics are increased from 45000 GHz @ 14.7 GHz ($x=0$) to 150500 GHz @ 14.5 GHz ($x=0.15$) by replacing Al^{3+} with Zn^{2+} - Mn^{4+} . The positive frequency temperature coefficient additive TiO_2 is used to prepare the temperature stable $\text{Mg}_2\text{Al}_{3.7}(\text{Mn}_{0.5}\text{Zn}_{0.5})_{0.3}\text{Si}_5\text{O}_{18}$ - y wt% TiO_2 composite ceramic. The composite ceramic of $\text{Mg}_2\text{Al}_{3.7}(\text{Mn}_{0.5}\text{Zn}_{0.5})_{0.3}\text{Si}_5\text{O}_{18}$ - y wt% TiO_2 ($8.7 \text{ wt}\% \leq y \leq 10.6 \text{ wt}\%$) presents the near-zero frequency temperature coefficient at 1225 °C sintering temperature: $\epsilon_r = 5.68$, $Q \times f = 58040 \text{ GHz}$, $\tau_f = -3.1 \text{ ppm}/^\circ\text{C}$ ($y=8.7 \text{ wt}\%$) and $\epsilon_r = 5.82$, $Q \times f = 47020 \text{ GHz}$, $\tau_f = +2.4 \text{ ppm}/^\circ\text{C}$ ($y=10.6 \text{ wt}\%$). These findings demonstrate promising application prospects for 5G and future microwave and millimeter-wave wireless communication technologies.

Keywords: Cordierite; Microwave and millimeter-wave dielectric ceramics; 5G/6G communication; Infrared reflectance spectrum

1. Introduction

With the rapid development and deployment of 5G communication technology from 5G-Sub6GHz to 5G/6G-Sub100GHz till terahertz, microwave and millimeter-wave dielectric ceramic materials would have been widely used in 5G/6G communication systems as dielectric materials of the resonators, filters, duplexers, microwave strip, substrate, etc [1-3]. There are three key parameters to evaluate the performance of microwave dielectric ceramics, namely the relative permittivity (ϵ_r), the quality factor ($Q \times f$) and the temperature coefficient of resonance frequency (τ_f), which are closely related to the application field, loss and temperature stability [4]. Compared with centimeter-wave, decimeter-wave and meter-wave, the wavelength of millimeter-wave and terahertz is shorter. Therefore, it is not necessary to select materials with a high dielectric constant to reduce the size of devices. Meanwhile, 5G and 6G require the time delay of signal transmission response to be less than 1 and 0.1 ns, respectively. Because the time delay (t_d) in the dielectric resonator is proportional to the square root of ϵ_r , materials with a low dielectric constant are selected to reduce it according to the following relationship [5]:

$$t_d = L \frac{\sqrt{\epsilon_r}}{c} \quad (1)$$

where c represents the velocity of light and L is the signal transmission distance. Hence, the low-dielectric constant cordierite ($\text{Mg}_2\text{Al}_4\text{Si}_5\text{O}_{18}$) material will be the leading candidate for future 5G-Sub100GHz and 6G-terahertz communications [6].

There are two stable forms of cordierite structure: α -cordierite, which has a

hexagonal structure sintered at high-temperature (1550-1600 °C), and β -cordierite, which has an orthorhombic structure at relative low temperature (1350-1475 °C)^[7]. The orthorhombic β -cordierite is the most commonly synthesized cordierite. However, β -cordierite ceramics with higher sintered temperatures and lower $Q \times f$ values do not meet the requirements of millimeter-wave communication applications. In the years 2007-2010, H. Oshato *et al.* reported cordierite ceramic for microwave and millimeter-wave applications with $\epsilon_r = 6.19$, $Q \times f = 39000 \text{ GHz} \sim 99110 \text{ GHz}$, and $\tau_f = -32 \text{ ppm}/^\circ\text{C} \sim -34 \text{ ppm}/^\circ\text{C}$ ^[8-9]. Song *et al.* studied the relationship between the crystal structure of cordierite ceramics and their microwave dielectric properties from the viewpoint of hexagonal ring symmetry of inner tetrahedron $[\text{Si}_4\text{Al}_2\text{O}_{18}]$ and outer octahedron $[\text{Mg}_6\text{O}_{36}]$ ^[10-12]. The substitution of $(\text{Li}_{0.5}\text{Ga}_{0.5})^{2+}$ for Mg^{2+} in $\text{Mg}_2\text{Al}_4\text{Si}_5\text{O}_{18}$ ceramics has improved the microwave dielectric properties of cordierite ceramics^[13].

As is well known, the microwave dielectric properties of a material will be affected by changes in its overall structure caused by ion substitution or the filling of other elements. The majority of prior research has been focused on elemental substitution at the Mg^{2+} octahedron lattice site of cordierite and temperature stable adjustment complicated by the positive temperature coefficient of resonant frequency of TiO_2 ^[14-16]. However, complex ionic modification of $[\text{AlO}_4]$ ionic lattice sites in cordierite is the subject of very few studies. Herein, in order to further explore the influence of complex ionic pairs coordinated replacing Al^{3+} tetrahedron lattice sites on cordierite dielectric ceramic, this paper designed a strategy of the substitution of $[\text{Mn}^{4+}_{1/2}\text{Zn}^{2+}_{1/2}]$ on Al^{3+} to prepare $\text{Mg}_2\text{Al}_{4-2x}(\text{Mn}_{0.5}\text{Zn}_{0.5})_{2x}\text{Si}_5\text{O}_{18}$ ($0 \leq x \leq 0.3$) solid solution ceramics, and then

further used TiO₂ to tune its temperature coefficient of resonant frequency. Compared to all previously reported data, a high $Q \times f$ value (150500 GHz) has been obtained for cordierite. Simultaneously, a series of wonderful temperature stable cordierite type ceramics have been developed with $\epsilon_r = 5.68 \sim 5.82$, $Q \times f = 47020 \text{ GHz} \sim 58040 \text{ GHz}$, $\tau_f = -3.1 \text{ ppm}/^\circ\text{C} \sim +2.4 \text{ ppm}/^\circ\text{C}$, which can be applied to future 5G and 6G communication applications with higher frequency.

2. Experimental procedure

Mg₂Al_{4-2x}(Mn_{0.5}Zn_{0.5})_{2x}Si₅O₁₈ cordierite-typed ceramics were prepared by high purity raw materials of MgO (99.99%), Al₂O₃ (99.99%), SiO₂ (99.99%), MnO₂ (99.5%), ZnO (99.99%), TiO₂ (99.99%). MgO and ZnO were calcined at 950 °C for 3 hours to exclude impurities, while the other raw materials were dried at 100 °C for 24 h to remove moisture. All raw materials were weighted according to the stoichiometric ratio and ball milled for 6 h with ethanol as the solvent in a Teflon tank. The dried powders were calcined at 1200 °C for 4 h, and the calcined powders were re-milled for 6 hours. The calcined powders were mixed with 8 wt% PVA solution and pressed into a cylindrical pellet of $\Phi 12 \text{ mm} \times 7 \text{ mm}$. Finally, the samples were sintered at 1250-1450 °C for 4 hours at a heating rate of 3 °C/min.

The bulk density (ρ_b) of ceramic samples was measured by the Archimedes method. The theoretical density can be obtained by the following formula:

$$\rho_{theo} = \frac{ZA}{V_c N_A} \quad (2)$$

where Z , A and V_c are the number of atoms in a unit cell, atomic weight and volume of

a unit cell, respectively. The relative density was obtained by the following formula:

$$\rho_r = \frac{\rho_b}{\rho_{theo}} \times 100\% \quad (3)$$

The crystalline structure of the sintered ceramic samples was identified by X-ray powder diffraction (XRD) using Cu K α radiation (Rigaku, Ultima IV, Japan) operated at 40 kV and 30 mA. The surface morphology of ceramic samples was examined using a scanning electron microscopy (SEM, Hitachi S-4800, Hitachi, Japan), which were thermal etched at the 100 °C lower than densification sintered temperature for 30 minutes. The infrared reflectance spectra were collected on the infrared beam line (IFS 66 v/S) of the Hefei National Synchrotron Radiation Laboratory. The microwave dielectric properties of the samples were measured by a Keysight E5071c network analyzer using the TE₀₁₈ mode dielectric resonator method. The temperature coefficients of resonance frequency (τ_f), were evaluated in the temperature range of 25-85 °C, calculated by the following formula:

$$\tau_f = \frac{f_2 - f_1}{f_1 \times (T_2 - T_1)} \times 10^6 (ppm/^\circ C) \quad (4)$$

where f_1 and f_2 were the resonant frequency at 25 and 85 °C, respectively.

3. Results and discussion

The bulk density of Mg₂Al_{4-2x}(Mn_{0.5}Zn_{0.5})_{2x}Si₅O₁₈ ($x=0, 0.05, 0.1, 0.15, 0.2, 0.25, 0.3$) ceramics at various sintering temperatures are shown in Figure 1(a). As x increases, the optimal sintering temperature decreases and the densification sintering range broadens up to 100 °C ($0.15 \leq x \leq 0.3$). The relative densities of each component are greater than 95% at optimal sintering temperature, as shown in Figure 1(b). The XRD

patterns of $\text{Mg}_2\text{Al}_{4-2x}(\text{Mn}_{0.5}\text{Zn}_{0.5})_{2x}\text{Si}_5\text{O}_{18}$ ceramics are shown in Figure(c). All XRD peaks of sintered samples are well matched with the orthorhombic phase of the cordierite structure (JCPDS No.82-1541) with the space group of $Cccm$ (66). Rietveld refinement was applied to the XRD data of the ceramic powder sample. Table S1 and S2 (Supporting Information) list the structural refinement data of all studied compositions. Figure S1 (Supporting Information) shows the Rietveld fitted pattern of $\text{Mg}_2\text{Al}_{4-2x}(\text{Mn}_{0.5}\text{Zn}_{0.5})_{2x}\text{Si}_5\text{O}_{18}$ ($x=0.15$). The low refinement factors ($R_{wp} = 8.56\%$, $R_p = 4.74\%$) indicate that the results of Rietveld refinement were reliable. The crystal structure schematic of $\text{Mg}_2\text{Al}_4\text{Si}_5\text{O}_{18}$ is shown in Figure 1(d).

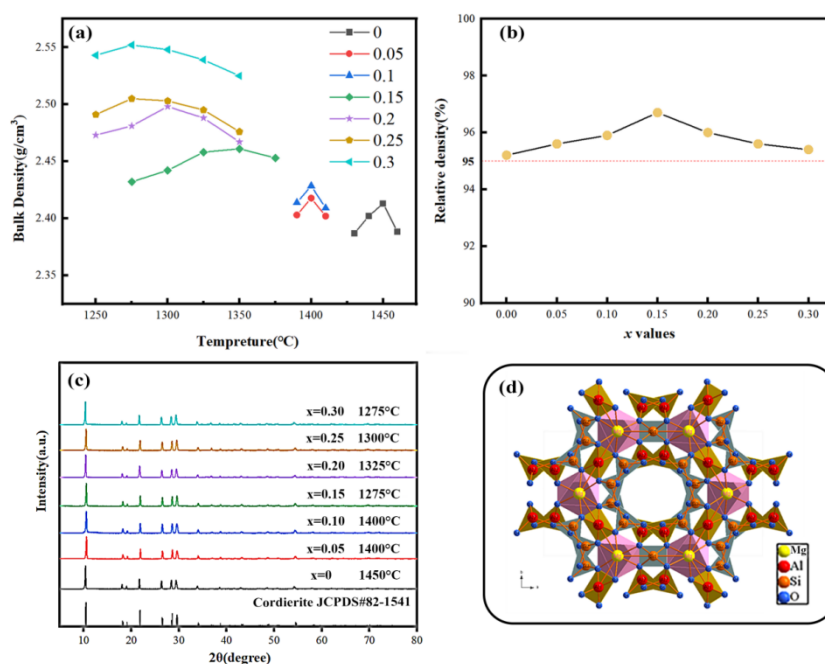


Figure 1. (a) The bulk density of $\text{Mg}_2\text{Al}_{4-2x}(\text{Mn}_{0.5}\text{Zn}_{0.5})_{2x}\text{Si}_5\text{O}_{18}$ ceramics as a function of sintering temperature. (b) The relative density of ceramics sintered with different components at the optimal sintering temperature. (c) XRD patterns of ceramics sintered with various components of $\text{Mg}_2\text{Al}_{4-2x}(\text{Mn}_{0.5}\text{Zn}_{0.5})_{2x}\text{Si}_5\text{O}_{18}$ at 1250-1450 °C for 4 h. (d)

The crystal structure schematic of $\text{Mg}_2\text{Al}_4\text{Si}_5\text{O}_{18}$ on the a-b plane.

The SEM images of $\text{Mg}_2\text{Al}_{4-2x}(\text{Mn}_{0.5}\text{Zn}_{0.5})_{2x}\text{Si}_5\text{O}_{18}$ ($x=0.1, 0.15, 0.2$) ceramics with various compositions at the optimal sintering temperature are presented in Figure 2. With the Zn^{2+} - Mn^{4+} doping concentration increasing, the grain size grows slightly and the porosity decreases. At $x=0.15$, a well-formed and dense microstructure is observed, which is consistent with the theoretical density variation trend in Figure 1(b). However, as the doping concentration increases, the porosity begins to increase, which can be attributed to the abnormal growth of certain grains.

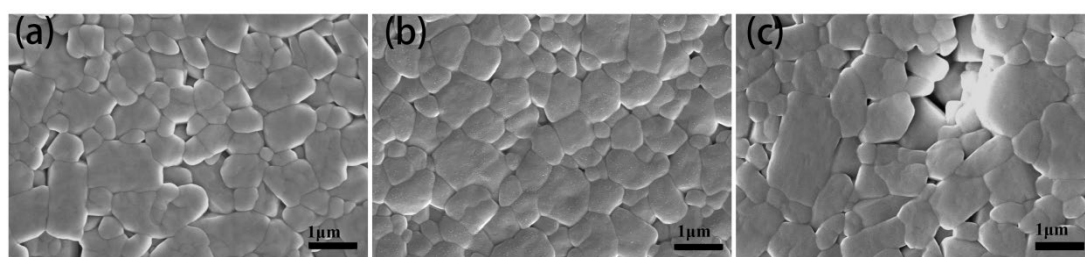


Figure 2. SEM images of the natural cross-sections of $\text{Mg}_2\text{Al}_{4-2x}(\text{Mn}_{0.5}\text{Zn}_{0.5})_{2x}\text{Si}_5\text{O}_{18}$ ceramics (a) $x=0.1$, (b) $x=0.15$, (c) $x=0.2$.

In order to explore the relationship between crystal structure and microwave dielectric properties, the complex chemical bond theory was used to elucidate the intrinsic factors affecting microwave dielectric properties of cordierite ceramics. The detailed calculation methods are included in the Supporting Information ^[17-22].

Figure 3 shows the ϵ_r , average bond ionicity and calculated permittivity (bar graph) of $\text{Mg}_2\text{Al}_{4-2x}(\text{Mn}_{0.5}\text{Zn}_{0.5})_{2x}\text{Si}_5\text{O}_{18}$ ceramics. We can see that ϵ_r firstly decreases and then increases, showing the same trend as average bond ionicity (A_{fi}). At $x=0.15$, ϵ_r and A_{fi} reach the minimum value at the same time, which indicates that ϵ_r and A_{fi} are strongly

correlated. The bar graph also displays the calculated permittivity (ϵ_c) results (4.95~4.963) according to the average bond ionicity, which are clearly close to the measured relative permittivity (ϵ_r).

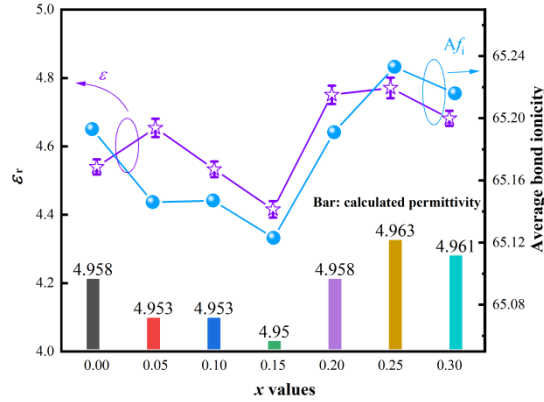


Figure 3. The ϵ_r , average bond ionicity and calculated permittivity of $Mg_2Al_{4-2x}(Mn_{0.5}Zn_{0.5})_{2x}Si_5O_{18}$ ceramics as a function of x value.

The correlation between the lattice energy U and inherent losses of microwave dielectric ceramics is strong as the U value reflects the ability of anions and cations to bind. Crystals with a greater binding capacity are more stable, which reduces their intrinsic losses. Therefore, U can be used to predict the $Q \times f$ value. As shown in Figure 4, the $Q \times f$ value of $Mg_2Al_{4-2x}(Mn_{0.5}Zn_{0.5})_{2x}Si_5O_{18}$ ceramics increases first with the increase of x , reaches a maximum at $x=0.15$, and then decreases gradually. The lattice energy reaches its maximum value of 117893 kJ/mol at the maximum $Q \times f$ value of 150500 GHz. In general, the $Q \times f$ value of ceramics is positively correlated with the lattice energy U .

Furthermore, the change in crystal structure is analyzed by calculating the degree of distortion of the $[Si_4Al_2O_{18}]$ six-membered ring. The lower standard deviation (σ) indicates less distortion. Six corners are taken as the internal angles of the hexagonal

six-membered ring as shown in Figure 1(d). In this paper, the Si-Al angles of [Si(2)–Al(2)–Si(3), Si(2)–Si(3)–Al(2), Si(3)–Si(2)–Al(2)] and the oxygen angle of [O(5)–O(4)–O(6), O(4)–O(6)–O(5), O(6)–O(5)–O(4)] were used to evaluate the standard deviation (σ) of the [Si₄Al₂O₁₈] six-membered ring. The formula 5 was used to calculate the σ values of the [Si₄Al₂O₁₈] ring:

$$\sigma = \sqrt{\frac{2 \times (a_1 - 120)^2 + 2 \times (a_2 - 120)^2 + 2 \times (a_3 - 120)^2}{6}} \quad (5)$$

where a_1 , a_2 , and a_3 are the three adjacent hexagonal angles in the six-membered ring. The detailed bond angles and calculated results are shown in Table S3 (Supporting Information). Figure 4 shows the σ of the [Si₄Al₂] ring and [O₆] ring as a function of x value. The fact that when $x=0.15$, the value is at its lowest and the $Q \times f$ value is at its highest indicates that the $Q \times f$ value of ceramics is inversely correlated with the angles of the six-membered ring.

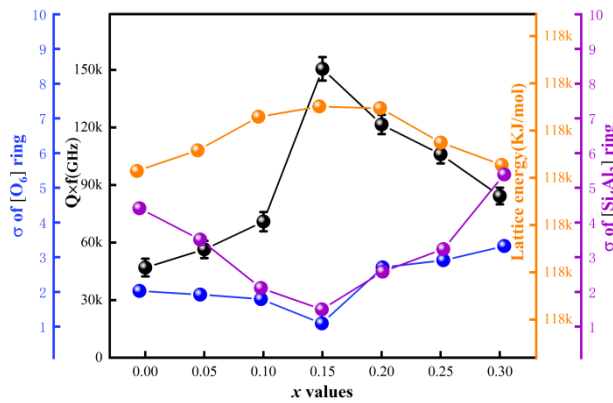


Figure 4. The $Q \times f$, lattice energy and σ of the [Si₄Al₂] and [O₆] ring of Mg₂Al_{4-2x}(Mn_{0.5}Zn_{0.5})_{2x}Si₅O₁₈ ceramics as a function of x value.

The bond energy E is a performance indicator for evaluating the strength of chemical bonds and structural stability. The greater the bond energy of a chemical bond, the greater the energy required to break it, and the greater the structural stability. The

fact that the average bond energy of the Mg-O bond is the largest when compared to the Si-O and Al-O bonds suggests that the Mg-O bond energy plays a major role in the temperature stability of cordierite. The τ_f value and the Mg-O bond energy of $\text{Mg}_2\text{Al}_{4-2x}(\text{Mn}_{0.5}\text{Zn}_{0.5})_{2x}\text{Si}_5\text{O}_{18}$ ceramics are shown in Figure 5. In this work, the τ_f value fluctuates from -25.3 to -38.2 ppm/°C. Similar variation trends between τ_f and the Mg-O bond energy can also be observed.

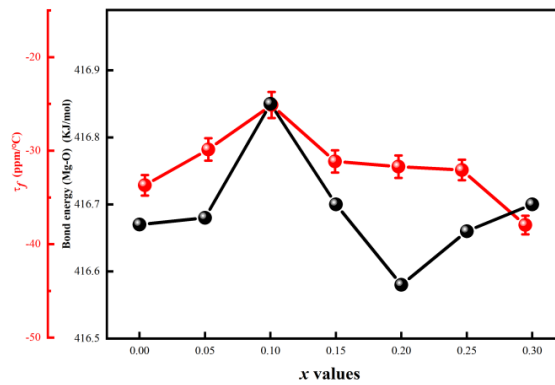


Figure 5. The τ_f value and the Mg-O bond energy of $\text{Mg}_2\text{Al}_{4-2x}(\text{Mn}_{0.5}\text{Zn}_{0.5})_{2x}\text{Si}_5\text{O}_{18}$ ceramics as a function of x .

Based on the optimal point of microwave dielectric properties at $x=0.15$, the temperature coefficient is modified. Figure 6 (a) shows the relationship between the bulk density and the sintering temperature of $\text{Mg}_2\text{Al}_{3.7}(\text{Mn}_{0.5}\text{Zn}_{0.5})_{0.3}\text{Si}_5\text{O}_{18-y}\text{TiO}_2$ ceramics. In comparison to pure cordierite ceramic, the addition of TiO_2 enables the production of well-compacted ceramics at a lower temperature of sintering. The bulk density of each group initially increases with the sintering temperature. When the maximum density is reached, the bulk density begins to decrease gradually. This may be the phenomenon of over-sintering. The maximum bulk density is 2.68 g/cm^3 at

1225 °C. Figure 6 (b) displays the XRD patterns of $\text{Mg}_2\text{Al}_{3.7}(\text{Mn}_{0.5}\text{Zn}_{0.5})_{0.3}\text{Si}_5\text{O}_{18-y}\text{TiO}_2$ ($y=0, 1.6, 3.3, 5.0, 6.8, 8.7, 10.6$ wt%) ceramics. With the increase of y , the TiO_2 diffraction peaks appear simultaneously with those of the cordierite phase at $y=1.6$ wt%.

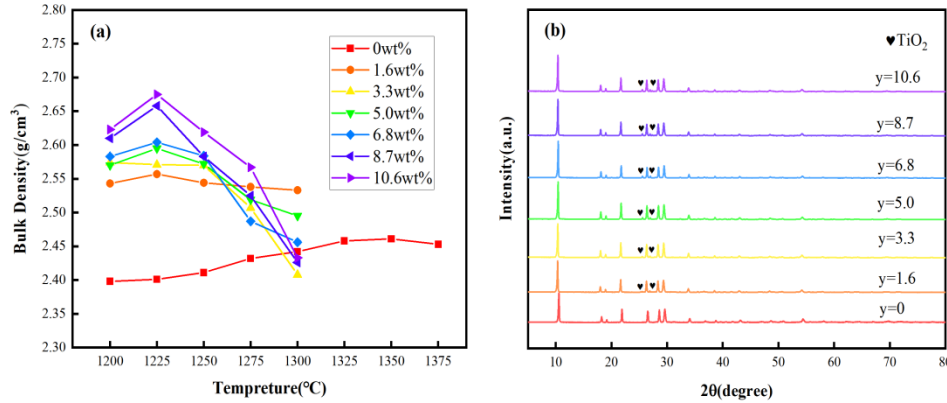


Figure 6. (a) The bulk density of $\text{Mg}_2\text{Al}_{3.7}(\text{Mn}_{0.5}\text{Zn}_{0.5})_{0.3}\text{Si}_5\text{O}_{18-y}\text{TiO}_2$ ($y=0, 1.6, 3.3, 5.0, 6.8, 8.7, 10.6$ wt%) ceramics as a function of sintering temperature. (b) XRD patterns of $\text{Mg}_2\text{Al}_{3.7}(\text{Mn}_{0.5}\text{Zn}_{0.5})_{0.3}\text{Si}_5\text{O}_{18-y}\text{TiO}_2$ ceramics.

Figure 7 shows the relationship between the microwave dielectric properties of $\text{Mg}_2\text{Al}_{3.7}(\text{Mn}_{0.5}\text{Zn}_{0.5})_{0.3}\text{Si}_5\text{O}_{18-y}\text{TiO}_2$ ($y=0, 1.6, 3.3, 5.0, 6.8, 8.7, 10.6$ wt%) ceramics. When $y=1.6$ wt%, a two-phase composite phenomenon occurs. Therefore, the composite rule can be used to predict the microwave dielectric properties of the two-phase composite ceramic. The dielectric constant and temperature coefficient of the resonance frequency were calculated by the compound formulas 6 and 7.

$$\ln \varepsilon_r = V_1 \ln \varepsilon_1 + V_2 \ln \varepsilon_2 \quad (6)$$

$$\tau_f = V_1 \tau_{f1} + V_2 \tau_{f2} \quad (7)$$

As y increases, the ε_r increases from 4.95 to 5.82 in Figure 7(a), which is caused by the addition of TiO_2 with higher ε_r . The red line represents the actual measured value,

and the blue line represents the calculated theoretical value. The $Q \times f$ value decreases from 150500 GHz to 47020 GHz in Figure 7(b), indicating that the addition of TiO_2 can increase dielectric loss ($\tan\delta$). The τ_f value is adjusted to near-zero (+2.4 ppm/°C) at $y=10.6$ wt%, which shows excellent temperature stability.

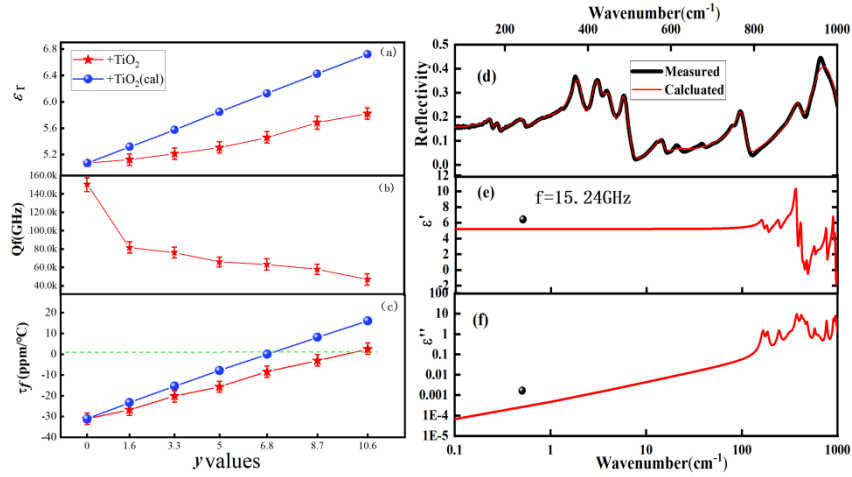


Figure 7. (a-c) Microwave dielectric properties of $\text{Mg}_2\text{Al}_{3.7}(\text{Mn}_{0.5}\text{Zn}_{0.5})_{0.3}\text{Si}_5\text{O}_{18-y}\text{TiO}_2$ ceramics as a function of TiO_2 weight fraction (y). (d) Experimental and fitted infrared reflection spectrum of $\text{Mg}_2\text{Al}_{3.7}(\text{Mn}_{0.5}\text{Zn}_{0.5})_{0.3}\text{Si}_5\text{O}_{18-y}\text{TiO}_2$ ($y=8.7$ wt%). (e-f) The complex dielectric constants in the microwave region.

To advance research into the intrinsic microwave dielectric properties of $\text{Mg}_2\text{Al}_{4-2x}(\text{Mn}_{0.5}\text{Zn}_{0.5})_{2x}\text{Si}_5\text{O}_{18}$ ceramics, their infrared reflectance spectra were analyzed using a classical harmonic oscillator model:

$$\varepsilon^*(\omega) - \varepsilon(\infty) = \sum_{j=1}^n \frac{(z_j e)^2 / m_j V_j \varepsilon_0}{\omega_{Tj}^2 - \omega^2 - i\omega\gamma_j} \quad (8)$$

The relevant parameters in the above formula are described in detail in the literature [23].

The relationship between complex reflectivity permittivity and $R(\omega)$ can be expressed as:

$$R(\omega) = \left| \frac{\sqrt{\varepsilon^*(\omega)} - 1}{\sqrt{\varepsilon^*(\omega)} + 1} \right|^2 \quad (9)$$

The infrared reflection spectrum can be well fitted with 14 modes in Figure 7 (d). Table S4 (Supporting Information) lists the relevant phonon parameters of $\text{Mg}_2\text{Al}_{3.7}(\text{Mn}_{0.5}\text{Zn}_{0.5})_{0.3}\text{Si}_5\text{O}_{18}$ -8.7wt% TiO_2 ceramic. Figure 7(e-f) presents the complex dielectric constants. The theoretical ε_r is 5.21 at 15.24 GHz, which is very close to the measured value of 5.68. It has been demonstrated that phonon absorption in the infrared region is the main reason for the dielectric polarization [24].

4. Conclusions

In this work, single-phase solid solution ceramics of $\text{Mg}_2\text{Al}_{4-2x}(\text{Mn}_{0.5}\text{Zn}_{0.5})_{2x}\text{Si}_5\text{O}_{18}$ ($0 \leq x \leq 0.3$) were prepared using a traditional solid-state reaction method. The correlation between bond ionicity, lattice energy, bond energy and microwave dielectric properties were analyzed through complex chemical bond theory and the σ values of $[\text{Si}_4\text{Al}_2\text{O}_{18}]$ six-membered ring. By fitting the infrared reflection spectrum, the theoretical ε_r was very close to the measured value. When sintered at 1350 °C, the composition of $x=0.15$ obtains the best microwave dielectric properties: $\varepsilon_r=4.53$, $Q \times f=150500$ GHz @ 14.5 GHz. The results prove that Zn^{2+} - Mn^{4+} can effectively improve the quality factor of cordierite ceramics without reducing the temperature stability, while also expanding their sintering range and decreasing their sintering temperature. Finally, temperature-stable composites of $\text{Mg}_2\text{Al}_{3.7}(\text{Mn}_{0.5}\text{Zn}_{0.5})_{0.3}\text{Si}_5\text{O}_{18}$ - $y\text{TiO}_2$ ($y=0, 1.6, 3.3, 5.0, 6.8, 8.7, 10.6$ wt%) ceramics were prepared by two-phase compounding with TiO_2 . When sintered at 1225 °C, the composition of $y=10.6$ wt% obtains the best microwave

dielectric properties: $\epsilon_r = 5.82$, $Q \times f = 47020$ GHz, $\tau_f = +2.4$ ppm/°C.

Acknowledgements

This work was supported by the National Natural Science Foundation of China under Grant No. 52161145401, and No. 51672063.

References

- [1] W. C. Lou, M. M. Mao, K. X. Song, K. W. Xu, B. Liu, W. J. Li, B. Yang, Z. M. Qi, J. W. Zhao, S. K. Sun, H. X. Lin, Y. Y. Hu, D. Zhou, D. W. Wang, I. M. Reaney, Low permittivity cordierite-based microwave dielectric ceramics for 5G/6G telecommunications, *J. Eur. Ceram. Soc.* 42 (2022) 2820-2826.
- [2] B. Liu, K. Sha, M. F. Zhou, K. X. Song, Y. H. Huang, C. C. Hu, Novel low- ϵ_r MGa₂O₄ (M = Ca, Sr) microwave dielectric ceramics for 5 G antenna applications at the Sub-6 GHz band, *J. Eur. Ceram. Soc.* 41 (2021) 5170-5175.
- [3] I. M. Reaney, D. Iddles, Microwave dielectric ceramics for resonators and filters in mobile phone networks, *J. Am. Ceram. Soc.* 89 (2006) 2063-2072.
- [4] F. F. Wu, D. Zhou, C. Du, B. B. Jin, C. Li, Z. M. Qi, S. K. Sun, T. Zhou, Q. Li, X. Q. Zhang, Design of a Sub-6 GHz Dielectric Resonator Antenna with Novel Temperature-Stabilized (Sm_{1-x}Bi_x)NbO₄ (x=0–0.15) Microwave Dielectric Ceramics, *ACS Appl. Mater. Interfaces.* 14 (2022) 7030-7038.
- [5] D. Xue, C. L. Sun, H. Y. Yang, L. Y. Yang, S. R. Zhang, Influence of Mg₂SiO₄ addition on crystal structure and microwave properties of

- Mg₂Al₄Si₅O₁₈ ceramic system, *J. Mater. Sci. Mater. Electron.* 29 (2018) 17967–17973.
- [6] T. Okamura, T. Kishino, Dielectric properties of rare-earth-added cordierite at microwave and millimeter wave frequencies, *Jpn. J. Appl. Phys.* 37 (1998) 5364–5366.
- [7] A. Miyake, Effect of the ionic size on thermal expansion of low cordierite by molecular dynamics simulation, *J. Am. Ceram. Soc.* 88 (2005) 121–126.
- [8] H. Ohsato, I. Kagomiya, M. Terada, K. Kakimoto, Origin of improvement of Q based on high symmetry accompanying Si-Al disordering in cordierite millimeter-wave ceramics, *J. Eur. Ceram. Soc.* 30 (2010) 315–318.
- [9] M. Terada, K. Kawamura, I. Kagomiya, K. Kakimoto, H. Ohsato, Effect of Ni substitution on the microwave dielectric properties of cordierite, *J. Eur. Ceram. Soc.* 27 (2007) 3045–3048.
- [10] K. X. Song, S. Wu, P. Liu, H. X. Lin, Z. H. Ying, P. Zheng, W. T. Su, J. X. Deng, L. Zheng, H. B. Qin, Phase composition and microwave dielectric properties of SrTiO₃ modified Mg₂Al₄Si₅O₁₈ cordierite ceramics, *J. Alloys Compd.* 628 (2015) 57–62.
- [11] K. X. Song, P. Liu, H. X. Lin, W. T. Su, J. Jiang, S. Wu, J. Wu, Z. H. Ying, H. B. Qin, Symmetry of hexagonal ring and microwave dielectric properties of (Mg_{1-x}Ln_x)₂Al₄Si₅O_{18+x} (Ln = La, Sm) cordierite-type ceramics, *J. Eur. Ceram. Soc.* 36 (2016) 1167–1175.
- [12] J. S. Wei, P. Liu, H. X. Lin, Z. H. Ying, P. Zheng, W. T. Su, K. X. Song, H. B. Qin,

- Crystal structure and microwave dielectric properties of CaTiO₃ modified Mg₂Al₄Si₅O₁₈ cordierite ceramics, *J. Alloys Compd.* 689 (2016) 81-86.
- [13] W. C. Lou, K. X. Song, F. Hussain, B. Liu, H. B. Bafrooei, H. X. Lin, W. T. Su, F. Shi, D. W. Wang, Bond characteristics and microwave dielectric properties of (Li_{0.5}Ga_{0.5})²⁺ doped Mg₂Al₄Si₅O₁₈ ceramics, *Ceram. Int.* 46 (2020) 28631-28638.
- [14] S. Wu, K. X. Song, P. Liu, H. X. Lin, F. F. Zhang, P. Zheng, H. B. Qin, Effect of TiO₂ doping on the structure and microwave dielectric properties of cordierite ceramics, *J. Am. Ceram. Soc.* 98 (2015) 1842-1847.
- [15] W. C. Lou, K. X. Song, F. Husain, A. Khesro, J. W. Zhao, H. B. Bafrooei, T. Zhou, B. Liu, M. M. Mao, K. W. Xu, E. Taheri-nassaj, D. Zhou, S. J. Luo, S. K. Sun, H. X. Lin, D. W. Wang, Microwave dielectric properties of Mg_{1.8}R_{0.2}Al₄Si₅O₁₈ (R= Mg, Ca, Sr, Ba, Mn, Co, Ni, Cu, Zn) cordierite ceramics and their application for 5G microstrip patch antenna, *J. Eur. Ceram. Soc.* 42 (2022) 2254-2260.
- [16] F. S. Wang, Y. M. Lai, Y. M. Zeng, F. Yang, B. Y. Li, X. Z. Yang, H. Su, J. Han, X. L. Zhong, Enhanced microwave dielectric properties in Mg₂Al₄Si₅O₁₈ through Cu²⁺ substitution, *Eur. J. Inorg. Chem.* 25 (2021) 2464-2470.
- [17] H. Y. Yang, S. R. Zhang, Y. W. Chen, H. C. Yang, Y. Yuan, E. Z. Li, Crystal chemistry, Raman spectra, and bond characteristics of trirutile-type Co_{0.5}Ti_{0.5}TaO₄ microwave dielectric ceramics, *Inorg. Chem.* 58 (2019) 968-976.
- [18] H. Li, X. Q. Chen, Q. Y. Xiang, B. Tang, J. W. Lu, Y. H. Zou, S. R. Zhang, Structure, bond characteristics and Raman spectra of CaMg_{1-x}Mn_xSi₂O₆ microwave dielectric ceramics, *Ceram. Int.* 45 (2019) 14160–14166.

- [19] H. Li, P. C. Zhang, S. Q. Yu, H. Y. Yang, B. Tang, F. H. Li, S. R. Zhang, Structural dependence of microwave dielectric properties of spinel structured $\text{Mg}_2(\text{Ti}_{1-x}\text{Sn}_x)\text{O}_4$ solid solutions: crystal structure refinement, Raman spectra study and complex chemical bond theory, *Ceram. Int.* 45 (2019) 11639-11647.
- [20] X. Q. Song, W. Z. Lu, Y. H. Lou, T. Chen, S. W. Ta, Z. X. Fu, W. Lei, Synthesis, lattice energy and microwave dielectric properties of $\text{BaCu}_{2-x}\text{Co}_x\text{Si}_2\text{O}_7$ ceramics, *J. Eur. Ceram. Soc.* 40 (2020) 3035-3041.
- [21] X. L. Shi, H. W. Zhang, D. N. Zhang, F. Xu, C. Liu, L. Shi, Y. H. Zheng, Structure and microwave dielectric properties of $\text{Li}_2\text{Mg}_3\text{Ti}_{1-x}(\text{Al}_{1/2}\text{Nb}_{1/2})_x\text{O}_6$ ceramics, *Ceram. Int.* 46 (2020) 13737-13742.
- [22] C. Y. Cai, X. Q. Chen, H. Li, J. Xiao, C. W. Zhong, S. R. Zhang, Microwave dielectric properties of $\text{Ca}_{1-x}\text{Sr}_x\text{MgSi}_2\text{O}_6$ ceramics, *Ceram. Int.* 46 (2020) 27679-27685.
- [23] D. Zhou, D. Guo, W. B. Li, L. X. Pang, X. Yao, D. W. Wang, I. M. Reaney, Novel temperature stable high- ϵ_r microwave dielectrics in the $\text{Bi}_2\text{O}_3\text{-TiO}_2\text{-V}_2\text{O}_5$ system, *J. Mater. Chem. C.* 23 (2016) 5357-5362.
- [24] H. H. Guo, D. Zhou, C. Du, P. J. Wang, W. F. Liu, L. X. Pang, Q. P. Wang, J. Z. Su, C. Singh, S. Trukhanov, Temperature stable $\text{Li}_2\text{Ti}_{0.75}(\text{Mg}_{1/3}\text{Nb}_{2/3})_{0.25}\text{O}_3$ -based microwave dielectric ceramics with low sintering temperature and ultra-low dielectric loss for dielectric resonator antenna applications, *J. Mater. Chem. C.* 14 (2020) 4690—4700.